EXPERIMENTAL INVESTIGATIONS ON THE INFLUENCE OF CUTTING AND TOOL GEOMETRY PARAMETERS OVER THE MACHINABILITY OF AISI 52100 STEEL IN HARD TURNING

Umamaheswarrao Ponugoti[1, 2], Ranga Raju Dantuluri[3], Naga Sai Suman Koka[1], Ravi Sankar Bhuvanagiri[2]

[1]Department of Mechanical Engineering, Andhra University College of Engineering, Visakhapatnam, A.P India PIN-530003
[2]Department of Mechanical Engineering, Bapatla Engineering College, Bapatla, A.P. India PIN-522102
[3]Department of Mechanical Engineering, Srinivasa Institute of Engineering & Technology, Amalapuram, A.P India PIN-533216

Corresponding author: Umamaheswarrao P, maheshponugoti@gmail.com

Abstract: The present work aims to study the behavior of AISI 52100 hard steel during turning with PCBN tools via investigations on machining force, surface roughness and workpiece surface temperature with variable speed, feed, depth of cut, nose radius and negative rake angle. Experimentation is executed as per Central Composite Design (CCD) of Response Surface Methodology (RSM). The dependency of responses on input parameters is articulated by non-linear regression equation. The parametric effects and their interactions were discussed using main effects plot and response surface plots. Results revealed that nose radius displays maximum effect on machining force followed by feed and negative rake angle. Surface roughness was mainly influenced by depth of cut, speed and nose radius subsequently feed. The depth of cut and nose radius has significant effect on workpiece surfae temperature (WST) followed by speed. Confirmation tests demonstrated the correctness of the methodology adopted and executed.

Key words: AISI 52100 steel; Machining force; Surface roughness; Workpiece surface temperature; Hard turning; Response surface method.

1. INTRODUCTION

Steels found sundry applications in manufacturing sector owing to their exceptional properties. The finishing process which effect productivity would be critical in ensuring the quality of the product, usually grinding and polishing operations are rendered for this purpose. However, the existing end processes were reinstated for harder materials by the turning termed as hard turning and proved success [1-4]. Hard turning is capable of manufacturing a complex geometry in one set up. It has got more flexibility compared to grinding. Hard machining characterizes improved material removal rate and reduction in machining time, resulting 30% off in machining cost contrast to grinding [5].

However, the investigation on the impact of cutting parameters over the machining performance was the ever constant endeavor in the field of manufacturing. The machinability studies on AISI 52100 steel was great interest due to its applicability in various components such as an axle, roller bearing, ball bearings, shear blades, spindle etc [6, 7].

Earlier studies on turning of AISI 52100 hard steel with CBN tools revealed that feed rate and cutting speed intensely influenced surface roughness and tool life, cutting forces are highly affected by depth of cut contrasted to feed rate and cutting speed [8, 9]. The similar trend was observed while hard turning of 100Cr6 material with coated mixed oxide ceramic inserts [10]. Nose radius was reported to be the dominating parameter [11, 12] and the same was observed with Al_2O_3 + TiC mixed ceramic tool [13], coated carbide tool [14, 15], TiN coated mixed oxide ceramic insert [16], tungsten carbide tool [17] and alumina, titanium-carbide composite tool [18].

Meddour et al. [19] reported that in AISI 52100 steel hard turning (HT) using a ceramic tool force was significantly sensitized by the depth of cut and surface roughness was notably improved at small feed and higher nose radius. Dilbag Singh and Venkateswara Rao [20] stated that feed was the dominant factor for surface finish afterwards nose radius in AISI 52100 steel turning. Suhail et al. [21, 22] noticed that greater the WST better the surface roughness obtained for AISI 1020 steel. The cutting execution could be successfully detected and constrained by the WST. While hard turning of AISI D2 steel cutting speed, depth of cut followed by feed were the major contributors to WST development [23, 24]. The WST was altogether influenced by feed pursued by cutting speed and depth of cut in turning of EN-9 steel [25].

From the literature, it was elucidated that hard turning was the best alternative to grinding owing to its merits. Much emphasis was made on AISI 52100 steel hard tuning by several researchers due to its applications in various parts of industry. The past studies made a large amount of interest to explore the influence of cutting parameters on the responses. Scanty literature was available on the effect of tool geometry parameters on the responses and the much interest was focused on nose radius. Most of the studies focused on the forces developed and surface roughness when hard turning. However, the WST reported to be the sensible and controlling factor for turning performance. Hence, the present study was aimed to conduct AISI 52100 steel hard turning with PCBN tools with cutting speed, feed rate and depth of cut as cutting conditions, nose radius and negative rake angle as tool geometry parameters. Machining force, surface roughness, and WST were considered as responses.

2. EXPERIMENTAL DETAILS

Kirloskar Turn master-35 type lathe was deployed for conducting experiments in dry condition. Experimental setup was depicted in Figure 1. Cylindrical bar of 500mm length, 48mm diameter with a hardness of 57 HRC made of AISI 52100 Steel used for the experiment. Machining length of work piece was fixed at 30mm for every experimental run. In the current work PCBN inserts (Figure 2) were used with varied nose radii such as r = 0.4mm, 0.6mm, 0.8mm, 1mm and 1.2mm with dissimilar negative rake angles (-5, -15, -25, -35 and -45) and ISO geometric designations (CNMG 120404, CNMG 120406, CNMG 120408, CNMG 120410 and CNMG 120412). The cutting forces were measured with Kistler three-component dynamometer, Surface roughness tester (SJ-210) was used to measure surface roughness and WST was measured using an infrared thermometer manufactured by AMPROBE (Range: -50^{o}C to 1550^{o}C, Model: IR 750).

Fig. 1. Experimental setup

Cutting and tool geometry parameters were varied at five levels throughout hard turning, and their impacts on responses like machining forces, surface roughness, and WST were examined. Factors and their levels are depicted in Table 1. A total of 32 experimental runs are conducted as per CCD of RSM shown in Table 2.

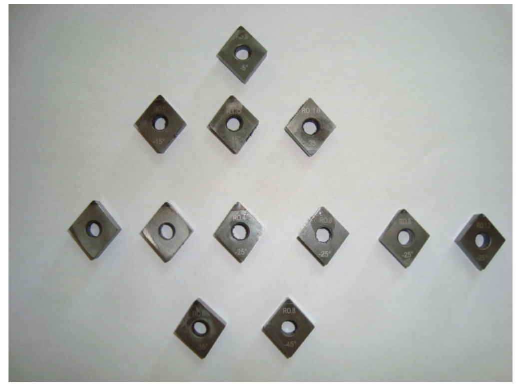

Fig. 2. PCBN Tools

Table 1. Factors and levels

Factors	Notation	Levels				
		-2	-1	0	1	2
Speed [rpm]	ν	200	400	600	800	1000
Feed [mm/rev]	f	0.02	0.04	0.06	0.08	0.1
Depth of Cut [mm]	d	0.4	0.5	0.6	0.7	0.8
Nose radius [mm]	r	0.4	0.6	0.8	1	1.2
Negative Rake angle [^{o}]	α	-5	-15	-25	-35	-45

2.1 Response surface methodology (RSM)

RSM was adopted for modeling and analysis of process parameters. In the RSM, the relation between response (Y) and input variables can be characterized as follows, equation (1) and equation (2):

$$Y = F(X_1, X_2, X_3.......) \quad (1)$$

$$Y = a_0 + \sum_{i=1}^{4} a_i X_i + \sum_{i=1}^{4} a_i X_i^2 + \sum_{i=1}^{4} a_{ij} X_i X_j \quad (2)$$

2.2 Statistical analysis of the responses

In order to understand the turning process, mathematical models were developed using the experimental results and RSM.

The relation between responses and input parameters can be expressed as:

$$Response = f(\nu, f, d, r, \alpha) \quad (3)$$

Table 2. Experimental matrix with responses

Exp. No	ν [rpm]	f [mm/rev]	d [mm]	r [mm]	α [°]	F_m [N]	Ra [μm]	WST [°C]
1	400	0.04	0.5	0.6	35	404.735	0.525	57.43
2	800	0.04	0.5	0.6	15	233.475	0.465	74.4
3	400	0.08	0.5	0.6	15	322.117	0.453	65.19
4	800	0.08	0.5	0.6	35	473.03	0.545	77.68
5	400	0.04	0.7	0.6	15	317.493	0.552	71.96
6	800	0.04	0.7	0.6	35	376.384	0.507	82.88
7	400	0.08	0.7	0.6	35	583.032	0.539	70.27
8	800	0.08	0.7	0.6	15	380.407	0.471	65.48
9	400	0.04	0.5	1	15	273.585	0.485	66.3
10	800	0.04	0.5	1	35	425.463	0.401	66.3
11	400	0.08	0.5	1	35	561.163	0.507	84.38
12	800	0.08	0.5	1	15	350.276	0.502	80.11
13	400	0.04	0.7	1	35	443.782	0.508	67.07
14	800	0.04	0.7	1	15	323.621	0.408	80.3
15	400	0.08	0.7	1	15	411.791	0.604	68.76
16	800	0.08	0.7	1	35	523.367	0.498	76.5
17	200	0.06	0.6	0.8	25	430.828	0.559	66.61
18	1000	0.06	0.6	0.8	25	355.441	0.456	82.73
19	600	0.02	0.6	0.8	25	309.595	0.468	70.85
20	600	0.1	0.6	0.8	25	534.481	0.53	74.88
21	600	0.06	0.4	0.8	25	344.431	0.45	71.39
22	600	0.06	0.8	0.8	25	449.219	0.48	74.2
23	600	0.06	0.6	0.4	25	359.396	0.514	67.18
24	600	0.06	0.6	1.2	25	446.225	0.485	76.05
25	600	0.06	0.6	0.8	5	279.954	0.484	70.32
26	600	0.06	0.6	0.8	45	601.276	0.509	73.68
27	600	0.06	0.6	0.8	25	358.525	0.507	68.6
28	600	0.06	0.6	0.8	25	370.743	0.518	74.94
29	600	0.06	0.6	0.8	25	378.525	0.52	71.41
30	600	0.06	0.6	0.8	25	403.976	0.512	66.36
31	600	0.06	0.6	0.8	25	380.24	0.488	76
32	600	0.06	0.6	0.8	25	370.65	0.522	69

Modeling is performed with response surface methodology. The Regression coefficients are estimated for responses and the modeling is done considering 95% confidence level and hence those terms having P value >0.05 are insignificant. The adequacy of the developed model is judged by the R^2 value and its value beyond 0.75 indicates the model is in good agreement [26]. Further, the observations are made with the aid of main effects plot and response surface plots.

3. RESULTS AND DISCUSSION

AISI 52100 steel hard turning was performed using PCBN inserts. The experiments were designed as per CCD and experimental runs along with responses were depicted in Table 2. Investigations on the effect of input parameters on output responses were carried out using RSM.

3.1 Analysis of machining force

The estimated regression coefficients for machining force and their quoted significances are depicted in Table 3.

Quadratic equation for machining force after eliminating insignificant terms is shown in equation (4).

R^2 value of 98.4% specifies that the model is in good agreement. From the ANOVA it is witnessed that machining force is significantly affected by nose radius followed by feed, negative rake angle, depth of cut and speed. ANOVA for machining force is given away in Table 4.

From the main effects plot (Figure 3) shows that machining force increases considerably with feed and negative rake angle whereas increment is marginal with the depth of cut and nose radius the similar trend was observed by Qian and Hossan & Dureja et al. [27, 28]. However, machining force decreases with an increase in speed. optimum machining force could be achieved in the following parametric level combination speed = 1000rpm, feed 0.02mm/rev, depth of cut 0.4mm, nose radius 0.4mm, negative rake angle 5° and the same was proved with the confirmation test given in Table 5.

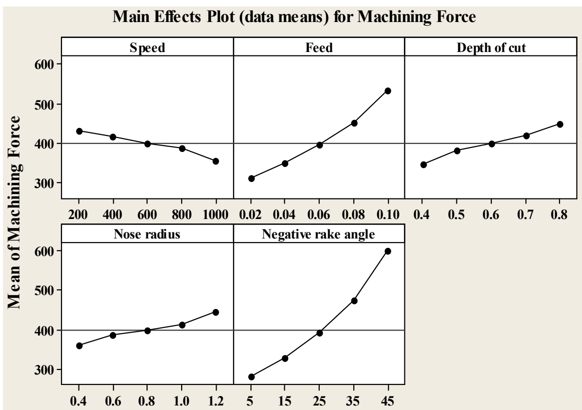

Fig. 3. Main effects plot for Machining force

The interaction effects from the Figure 4 shows that machining force decreases as speed increases irrespective of the variation in other parameters proving the contribution of thermal softening of material [29-31]. Higher machining forces are observed at upper limits of the speed vs other factors, while lower machining forces are noticed at the upper limit of speed and lower limits of feed, depth of cut and nose radius, at lower limits of negative rake angle and speed. However, the interaction is found to be more significant between speed and nose radius, at the lower limit of nose radius the machining force reduces steeply whereas the trend is not similar at its upper limit. Machining force rises with an increase in feed during interaction with the other parameters confirming the effect of cutting resistance and ploughing [32, 33]. Depth of cut shows considerable interaction with nose radius compared to other parameters, an increase in depth of cut leads to displacement of chipping away from nose radius [32, 34]. The interaction among nose radius vs speed and depth of cut was significant. At lower speeds domination of radial forces due to an increase in nose radius leads to elevated machining force [28]. Whereas enhancement in the cutting resistance owing to the increase of depth of cut dominates the radial forces at the lower limit of nose radius led to enhancement in machining force [32]. Negative rake angle shows considerable interaction with the depth of cut among all. The machining force is lower at lower limits of depth of cut and negative rake angle, increases steeply with the increase in negative rake angle at lower depth of cut due to the development of compressive stress state and stronger edge formation [27, 32]. Whereas the rise in machining force at higher limits of depth of cut was not similar to that of lower limits owing to the augmented cutting resistance. Higher machining forces are noticed during the interaction of parameters at their upper limits, however, for speed, it is at lower limit due to trivial thermal softening. Lower machining forces are noticed at lower limits feed and other parameters except speed during their interaction.

3.2 Analysis of Surface Roughness

The Estimated Regression Coefficients for surface roughness and their quoted significances are shown in Table 6. Quadratic equation for surface roughness after eliminating insignificant terms is shown in equation (5).

R^2 value of 97.5% indicates that the model is in good agreement. From the ANOVA it is observed that surface roughness is significantly affected almost equally by speed, depth of cut and nose radius followed by feed. However, the effect of negative rake angle is marginal. ANOVA for surface roughness is presented in Table 7.

From the main effects plot (Figure 5) it is noticed that surface roughness steeply falls as speed increases. This is caused by the elimination of built up edge [8, 32, 20] and lower deformation velocity due to increased thermal softening in turn, lateral plastic flow along the cutting edge minimizes leading to decrease in the peak-to-valley height of the surface irregularity [8] as a result surface roughness improves.

Surface roughness escalates with an increase in feed. This is due to the generation of feed marks on the surface of the workpiece and increased ploughing effect [35, 36]. A Similar trend was reported by the Lima et al. [36]. Surface roughness decreases with rise in nose radius of the tool the same was observed by Chou and Song & Dilbag Singh and Venkateswara Rao [18, 37]. Producing a better surface finish at a higher nose radius is well known in metal cutting [38]. Surface roughness rises with an increase in negative rake angle due to more edge strength and compressive stress state, similar results was reported by Suresh et al, Dilbag Singh and Venkateswara Rao [20, 32].

Table 3. Estimated Regression Coefficients for machining force

Term	Coef	SE Coef	T	P	Importance
Constant	380.627	7.473	50.931	0.000	Significant
ν	-31.871	7.649	-4.167	0.002	Significant
f	104.701	7.649	13.688	0.000	Significant
d	43.801	7.649	5.726	0.000	Significant
r	33.003	7.649	4.315	0.001	Significant
α	151.736	7.649	19.837	0.000	Significant
ν·ν	1.955	13.838	0.141	0.890	Insignificant
f·f	30.858	13.838	2.230	0.048	Significant
d·d	5.645	13.838	0.408	0.691	Insignificant
r·r	11.631	13.838	0.841	0.419	Insignificant
α·α	49.435	13.838	3.572	0.004	Significant
ν·f	-17.593	18.737	-0.939	0.368	Insignificant
ν·d	-18.241	18.737	-0.974	0.351	Insignificant
ν·r	24.122	18.737	1.287	0.224	Insignificant
ν·α	-39.316	18.737	-2.098	0.060	Insignificant
f·d	16.997	18.737	0.907	0.384	Insignificant
f·r	-11.589	18.737	-0.619	0.549	Insignificant
f·α	43.453	18.737	2.319	0.041	Significant
d·r	-32.971	18.737	-1.760	0.106	Insignificant
d·α	-47.921	18.737	-2.558	0.027	Significant
r·α	2.703	18.737	0.144	0.888	Insignificant

S = 18.74 R-Sq = 98.4% R-Sq (adj) = 95.6%

Table 4. ANOVA for machining force

Source	DF	SS	MS	% Contribution
ν	4	6286.6849	1571.6712	2.552578
f	4	67492.3953	16873.0988	27.40388
d	6	12367.3996	2061.2333	5.021525
r	10	101306.5389	10130.6539	41.13341
α	2	57673.3938	28836.6969	23.41708
Error	5	1161.2685	232.2537	0.471509
Total	31	246287.6810		

Table 5. Confirmation test for Machining force

Parametric levels	Machining force
speed 800rpm, feed 0.04mm/rev, depth of cut 0.5mm, nose radius 0.6mm, negative rake angle 15° (Expt. No-2)	233.475
speed 1000rpm, feed 0.02mm/rev, depth of cut 0.4mm, nose radius 0.4mm, negative rake angle 5°	213.281

Optimum surface roughness could be achieved in the following parametric level combinations speed 1000rpm, feed 0.02mm/rev, depth of cut 0.4mm, nose radius 1.2mm, negative rake angle 5° and the same was proved with the confirmation test given in Table 8. However, the interaction of speed results in marginal variation in surface roughness is observed at higher feed due to domination of feed marks [35], at lower limit of depth of cut due to the formation of lower built up edge due to lower uncut chip thickness and ploughing effect [38, 39], at higher negative rake angle due to augment in cutting forces [20] and at lower limits of nose radius from well known principles of metal cutting [38]. Lower surface roughness was noticed at combinations of at higher limits of speed Vs depth of cut and nose radius, higher limits of speed Vs lower limits of feed and negative rake angle.

The interaction effects from the Figure 6 shows that as speed increases surface roughness decreases due to the elimination of built up edge [8, 32, 20] and thermal softening of the material [29-31].

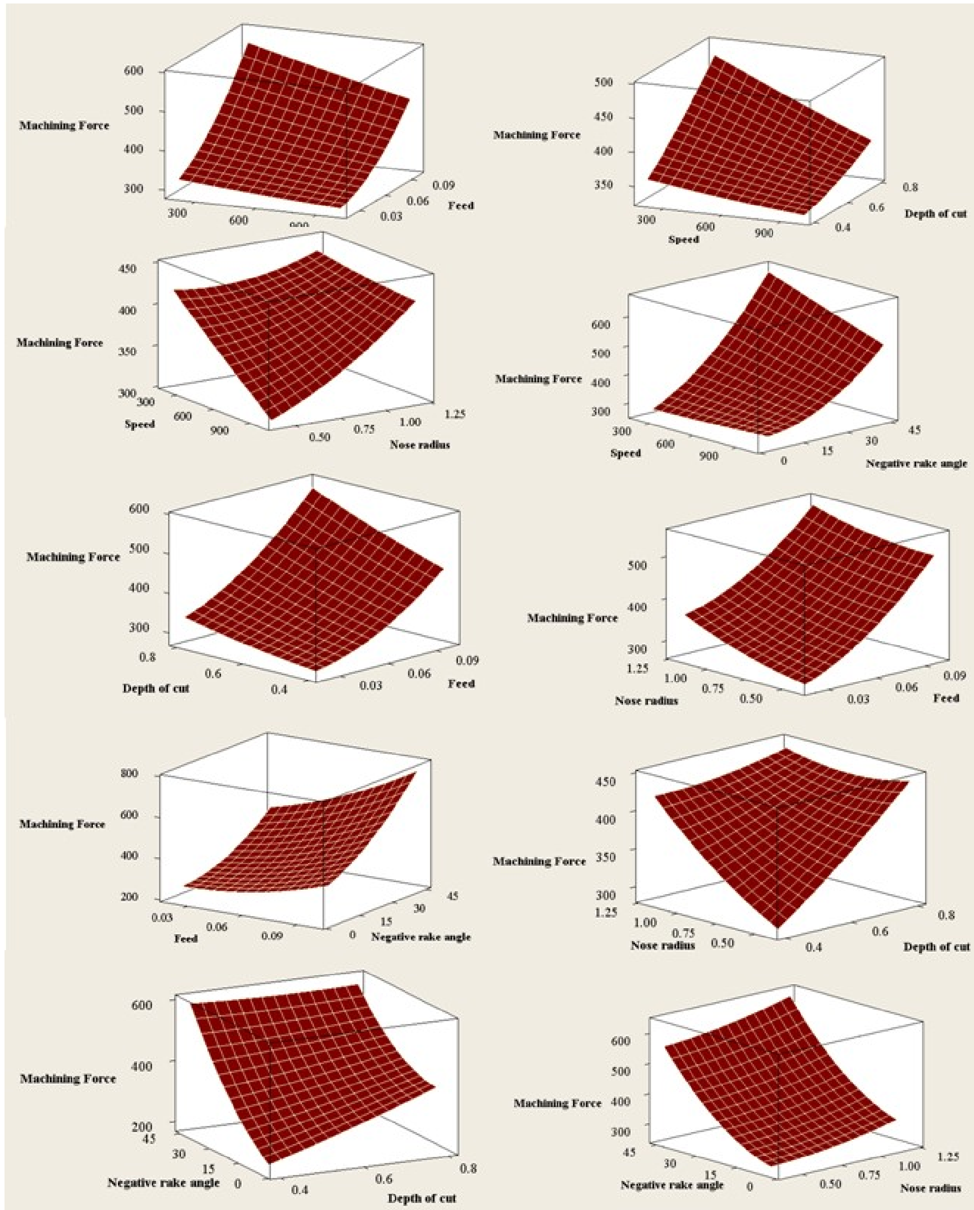

Fig. 4. Response surface plots for machining force

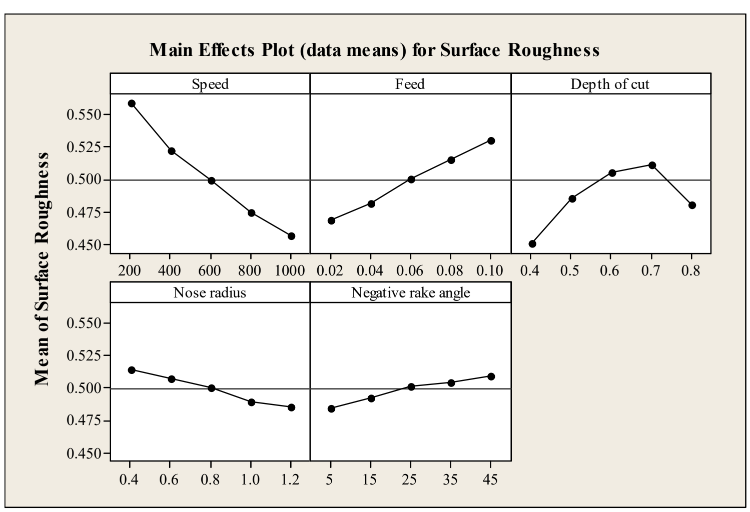

Fig. 5. Main effects plot for surface roughness

Table 6. Estimated Regression Coefficients for surface roughness

Term	Coef	SE Coef	T	P	Importance
Constant	0.509523	0.004426	115.127	0.000	Significant
ν	-0.048500	0.004530	-10.707	0.000	Significant
f	0.032667	0.004530	7.211	0.000	Significant
d	0.022000	0.004530	4.857	0.001	Significant
r	-0.016833	0.004530	-3.716	0.003	Significant
α	0.011667	0.004530	2.575	0.026	Significant
ν·ν	0.002909	0.008195	0.355	0.729	Insignificant
f·f	-0.005591	0.008195	-0.682	0.509	Insignificant
d·d	-0.039591	0.008195	-4.831	0.001	Significant
r·r	-0.005091	0.008195	-0.621	0.547	Insignificant
α·α	-0.008091	0.008195	-0.987	0.345	Insignificant
ν·f	0.050500	0.011096	4.551	0.001	Significant
ν·d	-0.065500	0.011096	-5.903	0.000	Significant
ν·r	-0.053500	0.011096	-4.822	0.001	Significant
ν·α	0.030000	0.011096	2.704	0.021	Significant
f·d	0.001500	0.011096	0.135	0.895	Insignificant
f·r	0.087500	0.011096	7.886	0.000	Significant
f·α	0.007000	0.011096	0.631	0.541	Insignificant
d·r	0.010500	0.011096	0.946	0.364	Insignificant
d·α	-0.014000	0.011096	-1.262	0.233	Insignificant
r·α	-0.065000	0.011096	-5.858	0.000	Significant

S = 0.01110 R-Sq = 97.5% R-Sq (adj) = 92.8%

Table 7. ANOVA for surface roughness

Source	DF	SS	MS	% Contribution
ν	4	0.0143	0.0036	26.93032
f	4	0.0090	0.0022	16.94915
d	6	0.0144	0.0024	27.11864
r	10	0.0141	0.0014	26.55367
α	2	0.0006	0.0003	1.129944
Error	5	0.0008	0.0002	1.506591
Total	31	0.0531		

Table 8. Confirmation test for Surface roughness

Parametric levels	Surface roughness
Speed 800 rpm, feed 0.04 mm/rev, depth of cut 0.5 mm, nose radius 1 mm, negative rake angle 35° (Expt. No-10)	0.401
speed 1000 rpm, feed 0.02 mm/rev, depth of cut 0.4 mm, nose radius 1.2 mm, negative rake angle 5°	0.372

$$\begin{aligned} Machining\ \ force &= -31.871\times \nu + 104.701\times f + 43.801\times d + 33.003\times r + 151.736\times \alpha \\ &+ 30.858\times f\times f + 49.435\times \alpha\times \alpha + 43.453\times f\times \alpha - 47.921\times d\times \alpha + 380.627 \end{aligned} \tag{4}$$

$$\begin{aligned} Surface\ roughness &= -0.048500\times \nu + 0.032667\times f + 0.022000\times d - 0.016833\times r + 0.011667\times \alpha \\ &- 0.039591\times d\times d + 0.050500\times \nu\times f - 0.065500\times \nu\times d - 0.053500\times \nu\times r + 0.030000\times \nu\times \alpha \\ &+ 0.087500\times f\times r - 0.065000\times r\times \alpha + 0.509523 \end{aligned} \tag{5}$$

$$\begin{aligned} WST &= 7.0442\times \nu + 2.4825\times f + 3.5142\times r - 7.4875\times \nu\times f - 16.0325\times f\times d + 9.4575\times f\times r \\ &+ 12.1425\times f\times \alpha + 71.2399 \end{aligned} \tag{6}$$

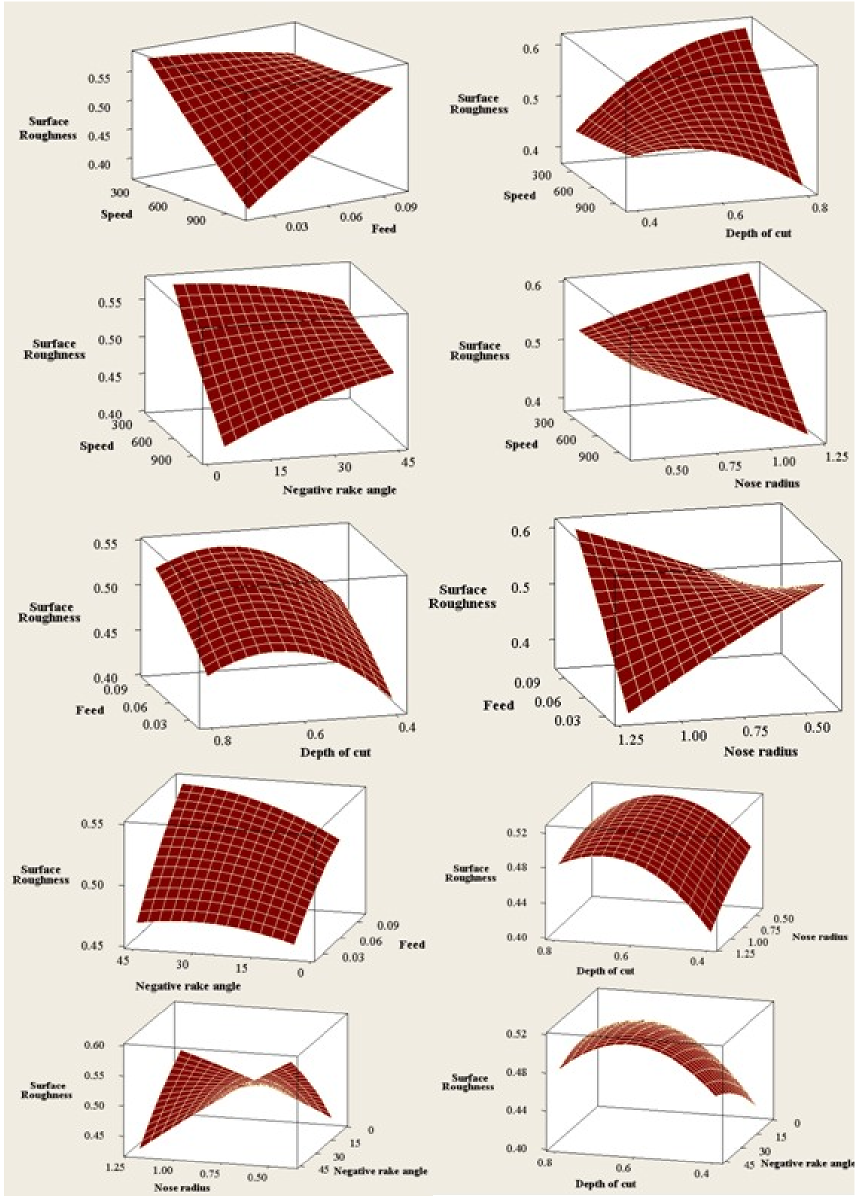

Fig. 6. Response surface plots of surface roughness

3.3 Analysis of workpiece surface temperature

The estimated regression coefficients for WST and their quoted significances are depicted in Table 9.

It is clear that the R^2 value is 92.8% indicates that the model is in good agreement. From the ANOVA it is observed WST is significantly affected by nose radius, speed, and depth of cut followed by feed. The nominal influence is observed for negative rake angle. ANOVA for WST is depicted in Table 10.

From the main effects plot (Figure 7) it is clear that WST increases with an increment in cutting parameters [22, 40] the similar observations were made by Suhail et al. [22, 40]. This is attributed to the more thermal acquisition on the surface [41] and ploughing effect. However, the increment in the WST is observed to be marginal with feed and negative rake angle.

It is also noticed that optimum WST could be achieved in the following parametric level combinations speed 1000rpm, feed 0.1mm/rev, depth of cut 0.8mm, nose radius 1.2mm, negative rake angle 45° and the same was proved with the confirmation test given in Table 11.

From the response plots (shown in Figure 8) it is evident that higher WST was noticed at the interaction of upper limits of all the parameters and this is attributed to the increased heat accumulation on the surface with an increase in speed, ploughing energy at peak feed & nose radius, cutting resistance at elevated depth of cut and compressive stress & harder cutting edge at higher negative rake angle.

Table 9. Estimated Regression Coefficients for WST

Term	Coef	SE Coef	T	P	Importance
Constant	71.2399	1.097	64.950	0.000	Significant
ν	7.0442	1.123	6.275	0.000	Significant
f	2.4825	1.123	2.211	0.049	Significant
d	1.4208	1.123	1.266	0.232	Insignificant
r	3.5142	1.123	3.130	0.010	Significant
α	1.3942	1.123	1.242	0.240	Insignificant
ν·ν	2.8655	2.031	1.411	0.186	Insignificant
f·f	1.0605	2.031	0.522	0.612	Insignificant
d·d	0.9905	2.031	0.488	0.635	Insignificant
r·r	-0.1895	2.031	-0.093	0.927	Insignificant
α·α	0.1955	2.031	0.096	0.925	Insignificant
ν·f	-7.4875	2.750	-2.723	0.020	Significant
ν·d	0.4775	2.750	0.174	0.865	Insignificant
ν·r	-4.7225	2.750	-1.717	0.114	Insignificant
ν·α	-0.9675	2.750	-0.352	0.732	Insignificant
f·d	-16.0325	2.750	-5.830	0.000	Significant
f·r	9.4575	2.750	3.439	0.006	Significant
f·α	12.1425	2.750	4.416	0.001	Significant
d·r	-5.0875	2.750	-1.850	0.091	Insignificant
d·α	2.6075	2.750	0.948	0.363	Insignificant
r·α	-3.1125	2.750	-1.132	0.282	Insignificant

S = 2.750   R-Sq = 92.8%   R-Sq (adj) = 79.6%

Table 10. ANOVA for WST

Source	DF	SS	MS	% Contribution
ν	4	315.4975	78.8744	27.45
f	4	96.4638	24.1159	8.39
d	6	282.5309	47.0885	24.58
r	10	375.8772	37.5877	32.7
α	2	6.9938	3.4969	0.60
Error	5	71.9653	14.3931	6.26
Total	31	1149.3284		

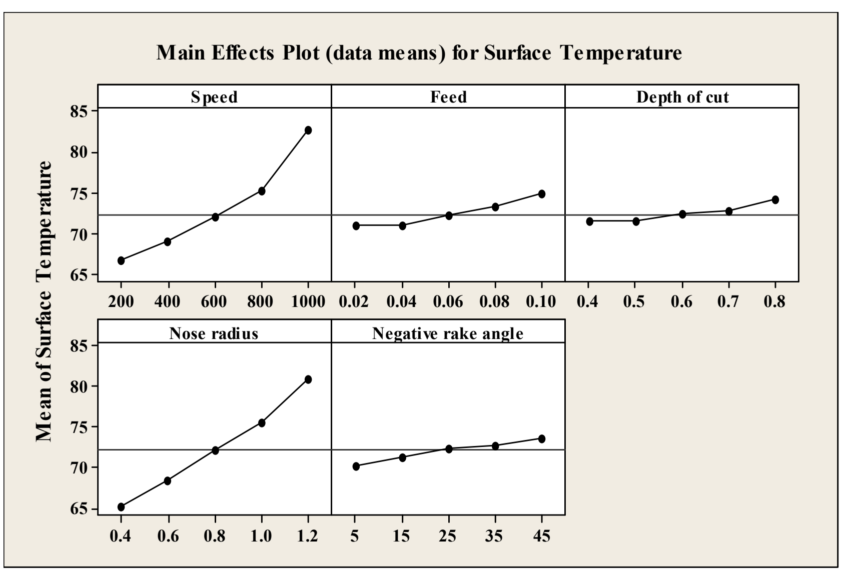

Fig. 7. Main effects plot for WST

Table 11. Confirmation test for WST

Parametric levels	Workpiece surface temperature
speed 400rpm, feed 0.08mm/rev, depth of cut 0.5mm, nose radius 1mm, negative rake angle 35° (Expt. No-11)	84.38
speed 1000rpm, feed 0.1mm/rev, depth of cut 0.8mm, nose radius 1.2mm, negative rake angle 45°	89.28

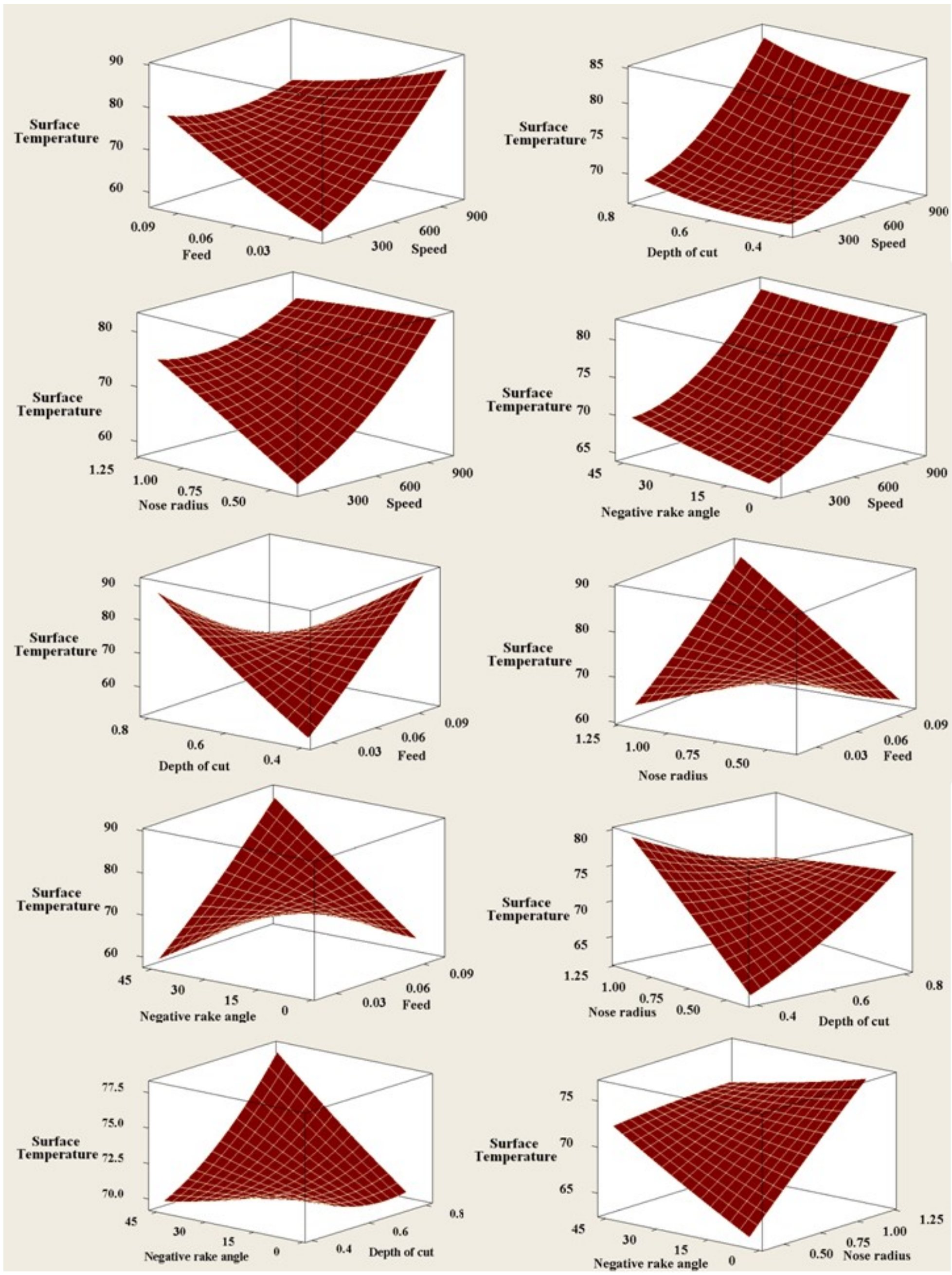

Fig. 8. Response surface plots for WST

4. CONCLUSIONS

In this paper, Investigations on AISI 52100 steel hard turning with PCBN tool was presented. The experiments were devised as per central composite design (CCD) of RSM. Effect of parameters on responses was presented with the aid of main effects plot and interaction effects were discussed with response surface plots.

Nose radius (41.13%) has a most notable effect on the machining force after that feed (27.4%), negative rake angle (23.41%), depth of cut (5.02%) and speed (2.55%). Depth of cut (27.11%), speed (26.93%) and nose radius (26.55%) almost has the same effect on surface roughness subsequently feed (16.94%). Negative rake angle effect was marginal. Nose radius (32.7%) has major influence on WST followed by speed (27.45%) and depth of cut (24.58%). Feed and negative rake angle have nominal influence. The parametric level combinations for optimum machining force, surface roughness and WST are identified from the respective main effects plots and confirmation tests are conducted for the individual responses.

Confirmation test yielded decrement of machining force & surface roughness by 8.64% & 7.79% respectively, whereas WST is increased by 5.48%. WST and surface roughness found interdependent and higher the WST yields better surface roughness. The interaction effects of machining parameters on the responses are discussed individually with the aid of response surface plots. Thermal softening at shear plane zone, cutting resistance, ploughing effect, uncut chip thickness and cutting edge strength plays vital role in effecting the responses and obviously varies with machining parameters.

5. ACKNOWLEDGEMENT

Authors are grateful to Karunya Institute of Technology and Sciences, Coimbatore for providing facilities.

6. NOMENCLATURE AND ABBREVIATIONS

PCBN - Polycrystalline cubic boron nitride
CCD - Central Composite Design of
RSM - Response Surface Methodology
AISI - American Iron and Steel Institute
CBN - cubic boron nitride
HT – Hard Turning
ANOVA - Analysis of Variance
HRC - Hardness on Rockwell ‘C’ Scale
DOE - Design of Experiments
WST-Workpiece surface temperature
R^2 - Coefficient of determination
DF - Degrees of freedom
SS - Sum of squares
MS - Mean of squares
ν - Speed
f - Feed
d- Depth of cut
r- Nose radius
α- Negative rake angle
F_m - Machining force

7. REFERENCES

1. König, W., Hochschule, T., Komanduri, R., Schenectady, D., Tönshoff, H.K., (1984). *Machining of hard materials,* Annals CIRP, **33**(2), 417–427.

2. König, W., Neises, A., (1993). *Wear mechanisms of ultrahard, nonmetallic cutting materials,* Wear, **162–164**, 12–21.

3. Tönshoff, H.K., Arendt, C., Amor, R.B., (2000). *Cutting of hardened steel,* Annals CIRP, **49**(2), 547–566.

4. Dogra, M., Sharma, V.S., Sachdeva, A., Suri, N.M., Singh, J. Dureja., (2010). *Tool Wear, Chip Formation and Work piece Surface Issues in CBN Hard Turning: A Review,* International Journal of Precision Engineering and Manufacturing, **11**(2), 341-358.

5. Huang, O.Y., Chou, Y.K., Liang, Y.S., (2007). *CBN tool wear in hard turning: a survey on research progresses,* International Journal of Advanced Manufacturing Technology, **35**, 443-453.

6. Li, C., Wang, J.L., (1993). *Effect of pre-quenching on martensite-bainitic microstructure and mechanical properties of GCr15 bearing steel,* Journal of Material Science, **28**(8), 2112-2118.

7. Umbrello, D., Hua, J., Shivpuri, R., (2004). *Hardness-based flow stress and fracture models for numerical simulation of hard machining AISI 52100 bearing steel,* Materials Science and Engineering A, **374**(1-2), 90-100.

8. Khamel, S., Ouelaa, N., Bouacha, K., (2012). *Analysis and prediction of tool wear, surface roughness and cutting forces in hard turning with CBN tool,* Journal of Mechanical Science and Technology, **26**(11), 3605-3616.

9. Bouacha, K., Yallese, M.A., Mabrouki, T., Rigal, J.F., (2010). *Statistical analysis of surface roughness and cutting forces using response surface methodology in hard turning of AISI 52100 bearing steel with CBN tool,* International Journal of Refractory Metals and Hard Materials, **28**, 349–361.

10. Vrabeľ, M., Maňková, I., Kovač, P., Beňo, J., Franková, M., Paľo, M., (2016). *Analysis and optimization of Hard Turning Process using Al_2O_3/TiCN Ceramic TiN PVD Coated Insert With Regard to Surface Roughness and Cutting Force Components,* Journal of Production Engineering, **19**(1), 22-26.

11. Ravi Sankar, B., Umamaheswarrao, P., (2017). *Analysis of Forces during Hard Turning of AISI 52100 Steel Using Taguchi Method,* Materials Today Proceedings, **4**, 2114–2118.

12. Ravi Sankar, B., Umamaheswarrao, P., Nawaz Sharief S.K., Suresh, T., Raju, R., (2017). *Parametric*

Investigations on Surface Roughness of Hard Turned AISI 52100 Steel, Applied Mechanics and Materials, **867**, 171-176.
13. Azizi, M.W., Belhadi, S., Yallese, M.A. et al. (2012). *Surface roughness and cutting forces modeling for optimization of machining condition in finish hard turning of AISI 52100 steel,* Journal of Mechanical Science and Technology, **26**(12), 4105-4114.
14. Shihab, S.K., Khan Z.A., Mohammad, A.A.S., Noor Siddiquee, A., (2014). *Optimization of surface integrity in dry hard turning using RSM,* Sadhana, Indian Academy of Sciences, **395**, 1035–1053.
15. Panda, A., Sahoo, A.K., Rout, A.K., (2017). *Machining Performance assessment of Hardened AISI 52100 steel using Multilayer coated carbide insert,* Journal of Engineering Science and Technology, **126**, 1488-1505.
16. Ildikó Maňková, Marek Vrabeľ, Jozef Beňo, Mária Franková, (2016). *Modelling and Analysis of Relationship between Cutting Parameters Surface Roughness and Cutting Forces using Response Surface Methodology when Hard Turning with Coated Ceramic Inserts,* Key Engineering Materials, **686**, 19-26.
17. Abhang, L.B., Hameedullah, M., (2012). *Optimal Machining Parameters for Achieving the Desired Surface Roughness in Turning of Steel,* The Journal of Engineering Research, **9**(1), 37-45.
18. Chou, Y.K., Song, H., (2004). *Tool nose radius effects on finish hard turning,* Journal of Materials Processing Technology, **148**, 259-268.
19. Meddour, I., Yallese, M.A., Khattabi, R., Elbah, M., Boulanouar, L., (2015). *Investigation and modeling of cutting forces and surface roughness when hard turning of AISI 52100 steel with mixed ceramic tool: cutting conditions optimization,* International Journal of Advanced Manufacturing Technology, **77**(5), 1387-1399.
20. Singh, D., Rao, P.V., (2007). *A surface roughness prediction model for hard turning process,* International Journal of Advanced Manufacturing Technology, **32**, 1115–1124.
21. Suhail Adeel, H., Ismail, N., Wong, S.V., Abdul Jalil, N.A., (2010). *Optimization of Cutting Parameters Based on Surface Roughness and Assistance of Work piece Surface Temperature in Turning Process,* American Journal of Engineering and Applied Sciences, **3**(1), 102-108.
22. Suhail Adeel, H., Ismail, N., Wong, S.V., Abdul Jalil, N.A., (2011). *Workpiece Surface Temperature for In-process surface roughness prediction using Response Surface methodology,* Journal of Applied sciences, **11**(2), 308-315.
23. Das, S.R., Nayak R.P., Dhupal, D., (2012) *Optimization of Cutting Parameters on Tool Wear, Work piece Surface Temperature and Material Removal Rate during Turning of AISI D2 Steel,* International Journal of Engineering Research & Technology, **1**(5), 1-10.
24. Das, S.R., Nayak R.P., Dhupal, D., (2012). *optimization of cutting parameters on tool wear and work piece surface temperature in turning of AISI D2 steel,* International Journal of Lean Thinking, **3**(2), 140-156.
25. Hardeep, S., Sumit, S., Vivek, A., Vineet, K., Sandeep, S., (2013). *Study of Cutting Parameters on Turning using EN9,* International Journal of Advance Industrial Engineering, **1**(2), 40-42.
26. Le Man, H., Behera, S.K., Park, H.S., (2010). *Optimization of operational parameters for ethanol production from Korean food waste leachate,* International Journal of Environmental Science and Technology, **7**(1), 157–164.
27. Qian, L., Hossan, M.R., (2007). *Effect on cutting force in turning hardened tool steels with cubic boron nitride inserts,* Journal of Materials Processing Technology, **191**(1–3), 274–278.
28. Dureja, J.S., Gupta, V.K., Sharma, V.S. et al. (2010). *Wear mechanisms of TiN-coated CBN tool during finish hard turning of hot tool die steel,* Proc IMechE, Part B: J Engineering Manufacture, **224**, 553–566.
29. Ebrahimi, A., Moshksar, M.M., (2009). *Evaluation of machinability in turning of micro alloyed and quenched tempered steels: tool wear, statistical analysis, chip morphology,* Journal of Materials Processing Technology, **209**, 910–921.
30. Lin, H.M., Liao, Y.S., Wei, C.C., (2008). *Wear behavior in turning high hardness alloy steel by CBN tool,* Wear, **264**, 679–684.
31. Yan, H., Hua, J., Shivpuri, R., (2005). *Numerical simulation of finish hard turning for AISI H13 die steel,* Science and Technology of Advanced Materials, **6**, 540-554.
32. Suresh, R., Basavarajappa, S., Gaitonde, V.N., Samuel, G.L., Paulo Davim, J., (2013). *State-of-the-art research in machinability of hardened steels,* Proceedings of the Institution of Mechanical Engineers, Part B: Journal of Engineering Manufacture, **227**(2), 191–209.
33. Lalwani, D.I., Mehta, N.K., Jain, P.K., (2008). *Experimental investigations of cutting parameters influence on cutting forces and surface roughness in finish hard turning of MDN250 steel,* Journal of Materials Processing Technology, **206**, 167–179.
34. Lin, Z.C., Chen, D.Y., (1995). *A study of cutting with CBN tool,* Journal of Materials Processing Technology, **49**, 149–164.
35. Azizi, M.W., Belhadi, S., Yallese, M.A., Lagred, A., Bouziane, A., Boulanouar, L., (2016). *Study of the machinability of Hardened 100cr6 Bearing Steel with TIN coated ceramic inserts,* Proceedings of Third International Conference on

Energy, Materials, Applied Energetics and Pollution ICEMAEP2016, pp. 171-175, Constantine, Algeria.
36. Lima, J.G., Avila, R.F., Abrao, A.M. et al. (2005). *Hard turning: AISI 4340 high strength low alloy steel and AISI D2 cold work tool steel,* Journal of Materials Processing Technology, **169**, 388–395.
37. Singh, D., Venkateswara Rao, P., (2007). *Optimization of Tool Geometry and Cutting Parameters for Hard Turning,* Materials and Manufacturing Processes, **22**, 15–21.
38. Trent, E.M., Wright, P.K., (2000). *Metal Cutting,* Fourth Edition, Butterworth-Heinemann, Boston.
39. Bartarya, G., Choudhury, S.K., (2012). *Effect of cutting parameters on cutting force and surface roughness during finish hard turning AISI52100 grade steel,* Procedia CIRP, 1651–1656.
40. Suhail Adeel, H., Ismail, N., Wong, S.V., Abdul Jalil, N.A., (2012). *Surface roughness identification using the grey relational analysis with multiple performance characteristics in turning operations,* Arabian Journal for Science and Engineering, **37**(4), 1111–1117.
41. Iurea, P., Carausu, C., Tampu, C., Chirita, B., Husanu, V., (2016), *Residual stresses generated a troughing grinding and hard turning of raceways of bearing rings*, International Journal of Modern Manufacturing Technologies, VIII (2), 19-24.

Received: January 7, 2020 / Accepted: June 15, 2020 / Paper available online: June 20, 2020